*17th World Conference on Earthquake Engineering, 17WCEE*
*Sendai, Japan - September 13th to 18th 2020*
*Paper N° C000585 (Abstract ID)*
*Registration Code: A01621*

# EXPERIMENTAL CHARACTERIZATION OF A TWO-STOREY STEEL FRAME EQUIPPED WITH CRESCENT-SHAPED BRACES

M. Palermo[(1)], V. Laghi[(2)], S. Silvestri[(3)], G. Gasparini[(4)], T. Trombetti[(5)]

[(1)] *Assistant professor, Department of Civil, Chemical, Environmental and Materials Engineering, University of Bologna, michele.palermo7@unibo.it*
[(2)] *Ph.D candidate, Department of Civil, Chemical, Environmental and Materials Engineering, University of Bologna, vittoria.laghi2@unibo.it*
[(3)] *Associate professor, Department of Civil, Chemical, Environmental and Materials Engineering, University of Bologna, stefano.silvestri@unibo.it*
[(4)] *Assistant professor, Department of Civil, Chemical, Environmental and Materials Engineering, University of Bologna, giada.gasparini4@unibo.it*
[(5)] *Associate professor, Department of Civil, Chemical, Environmental and Materials Engineering, University of Bologna, tomaso.trombetti@unibo.it*

## *Abstract*

The work provides the main results of an experimental campaign aimed at assessing the structural response of steel frame structures braced with so-called Crescent Shaped Braces (CSB) hysteretic devices. The CSB is a steel dissipative device having a kind of “boomerang” shape that connect two points of a structure (either two elements of the same floor, in a link-type configuration, or two different stories, in a brace-type configuration) The particular geometrical shape of the device is responsible of a specific non-linear behavior characterized by an elasto-plastic range followed by a final hardening, when subjected to traction, or by an elasto-plastic range followed by a slight softening, when subjected to compression. The insertion of ad-hoc designed CSB devices in not-moment resisting frames as diagonal braces allows to obtain an enhanced lateral resting system characterized by an optimized global force-displacement behavior capable of satisfying multiple seismic performance objectives. In previous investigations the behaviour of CSB have been investigated by means of analytical studies, numerical simulations and experimental tests on scaled (1:6) specimens. The objective of the paper is to provide the main experimental results and first interpretation of a series of tests conducted at the laboratory CIRI Buildings & Construction of the University of Bologna on a 1:2 scaled two-storey steel frame prototype structure incorporating diagonal CSB devices.
*Keywords: Earthquake-Resistant Design; Hysteretic dampers, Experimental tests.*

## 1. Introduction

Building structures are expected to guarantee safety requirements even under extreme events (such as rare earthquakes) to satisfy the society’s expectations. When dealing with seismic design, two main strategies can be envisaged to achieve the required safety levels: (i) guarantee a high ductility capacity to allow structures to exceed their elastic limit under severe earthquake; (ii) minimize the energy transmitted by the earthquake to the structural system, by means of seismic protection systems such as added dampers and base isolators.

In the first strategy, the exploitation of the full non-linear response of the structural elements provides advantages in terms of hysteretic energy dissipation, but, on the other hand, it also causes considerable damages on beams and columns, which therefore must be properly dimensioned and detailed in order to develop desired ductile mode of failure. Although this first strategy is associated with structural damages and associated economical direct and indirect losses [1], [2], (particularly noticeable during strong ground motions), it is a cost-effective strategy commonly adopted in seismic-resisting design.

In the second strategy, the introduction of a system of added dampers allows to maximize energy dissipations, thus reducing the amount of elastic energy to be absorbed by the structural elements. Although its high performances, this second strategy is more costly, thus usually adopted only for specific structures with high-risk destination use (i.e. strategic buildings for the society, such as hospitals, schools, fire and/or police stations, ...).
In light of this aspects, the use of low-cost hysteretic devices to obtain earthquake-resistant structures could lead to satisfy both the positive aspects of both strategies, i.e. concentration of damage on selected fusible low-cost elements and high hysteretic dissipation of earthquake-induced energy.
The Crescent-Shaped Brace (CSB) is a yielding steel element, recently proposed by the authors, which can be used to design seismic-resisting systems able to satisfy multiple performance objectives [3, 4] in the framework of Performance Based Seismic Design [5-7]. The CSB is characterized by a boomerang-like shape which provides the structure with both stiffness and hysteretic energy dissipation at the same time that can be tailored based on specific global geometrical parameters and cross-section properties. The CSB device was initially studied and proposed in scientific literature [4, 8] as an innovative seismic protection solution based on the concept of "shock-absorbing soft storey", originally proposed in the late 1960s by Khan and Fintel in 1968 [9]. Different applications have been explored, such as: (i) dissipative braces at each storey of frame structures; (ii) dissipative horizontal links for decks; (iii) semi-rigid connection at the hinged beam-column nodes [10, 11]. A first experimental campaign was carried out in 2017 on scaled (1:6) devices, and the results compared with analytical and numerical studies, confirming the expected dissipative capacity [10]. However, it becomes crucial to study the real performance of the brace when inserted within a frame structure and subjected to cyclic loading, as for the case of earthquake-induced action.

## 2. The Crescent Shaped Brace device

The Crescent Shaped Brace (CSB) is a boomerang-shaped steel element which connects two points of the structure [10-12]. It can be designed to achieve the desired combination of strength, stiffness, ductility and energy dissipation resulting from multiple performance objectives, within the context of PBSD [13].
Figure 1 presents the geometry and force-displacement response of a bi-linear symmetric CSB. The typical force-displacement relationships in tension and compression are governed by the interaction between the mechanical non-linearity of the material and the geometrical non-linearity due to the combination of axial force and bending moment depending on the variation of the lever arm d.

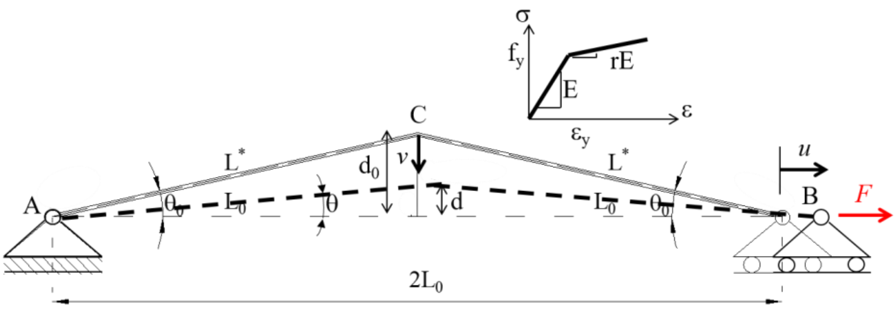


(a)



 

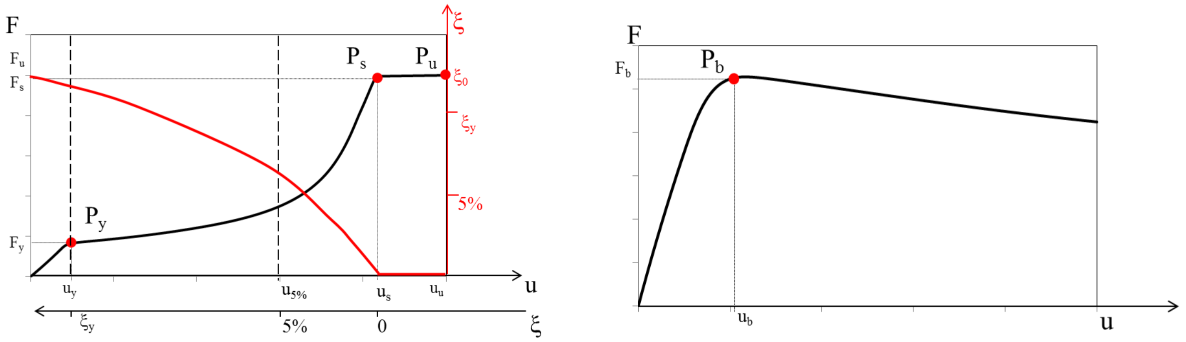


(b) (c)

Figure 1 – (a) The symmetric bilinear CSB; (b) typical lateral force-displacement response of the CSB in tension and (c) in compression.

In case of tension (Fig. 1b), the force-displacement relationship is typically constituted by an initial elastic phase until the first yielding point, occurring in the cross-section at the knee point, followed by a pseudo-plastic phase governed mainly by the mechanical behavior of the material, and a final hardening phase governed mainly by geometrical non-linearity. The initial elastic stiffness, the extent of the ductility plastic phase and the final hardening of the curve can be controlled by appropriately choosing the geometrical and mechanical parameters of the device [11]. The red curve in **Errore. L'origine riferimento non è stata trovata.**2a shows the variation of the normalized lever arm ξ (d/2L0) as a function of the lateral displacement u. It is possible to notice how the second order effects become significant approximately for ξ values smaller than 5%.
In case of compression (Fig. 1c), after a first elastic phase that ends with the achievement of yielding in the cross-section at the knee point, the curve presents a softening branch governed by geometric non-linearity.

## 3. Design of the prototype frame

With the aim of evaluating the experimental response of CSB when inserted in frame structures as diagonal braces, a prototype frame equipped with CSB has been designed and tested. The experimental tests are part of the regional TIRISICO project (POR-FESR 2014-20 program founded by Emilia-Romagna region, Italy).
In particular, two different configurations have been tested: (1) frame equipped with CSB device at the first storey only (Fig. 2a); (2) frame equipped with CSB devices at both storeys, placed along the same direction (Fig. 2b).
The prototype frame has been designed and realized in collaboration with Effebi company, while the tests have been carried out between December 2018 and February 2019 at CIRI Building & Construction laboratory of the University of Bologna. The prototype is a half-scaled two-storey one-bay steel frame, having a 2.6 m bay span and 1.6 m inter-storey height (representative of a typical structure for residential building).
To avoid early yielding in the columns and to allow the CSB element to carry the entire amount of horizontal force applied by the actuator, the frame has been pinned at the base with pinned connections made with M42 8.8 pins. The columns are unique elements from bottom to top realized with HEB140 European profiles. The beams are realized with coupled UPN200 Italian profiles chamfered at the corners. The CSB devices were realized with rectangular PL 120x30 cross-section elements. The initial lever arm of the device ($d_0$ = 200 mm) corresponds to $\xi_0$=10%. The columns have been anchored to the ground level with high resistance Dywidag bars. The connections between the columns, the beams and the diagonal CSBs have been realized with 30-mm thickness steel plates (welded to the columns) and M16 10.9 bolts (Figure 3).



 

The mechanical properties of the steel material adopted to realize the CSB devices were obtained by means of tensile tests performed on two prismatic samples having dimensions 30×30×358 mm$^3$, and instrumented with 2 strain gauges. A Universal machine of maximum load capacity of 400 kN was used for the test, imposing a speed of 10 MPa/s up to failure. The following mechanical properties were obtained: yielding stress $f_y$ = 326 MPa, yielding strain $\varepsilon_y$ = 0.168%, ultimate tensile strength $f_u$ = 465 MPa, strain to failure $\varepsilon_u$ = 29.67% and Young's modulus $E$ = 210700 MPa.

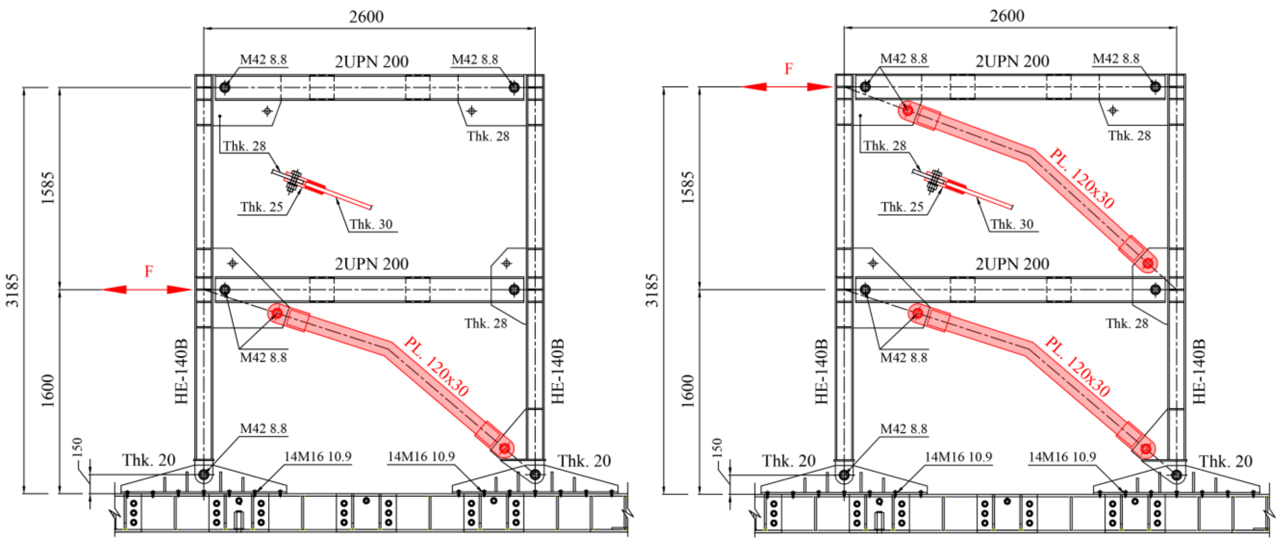


(a) (b)

Figure 2 - Test frame equipped with CSB devices: (a) Configuration 1; (b) Configuration 2.

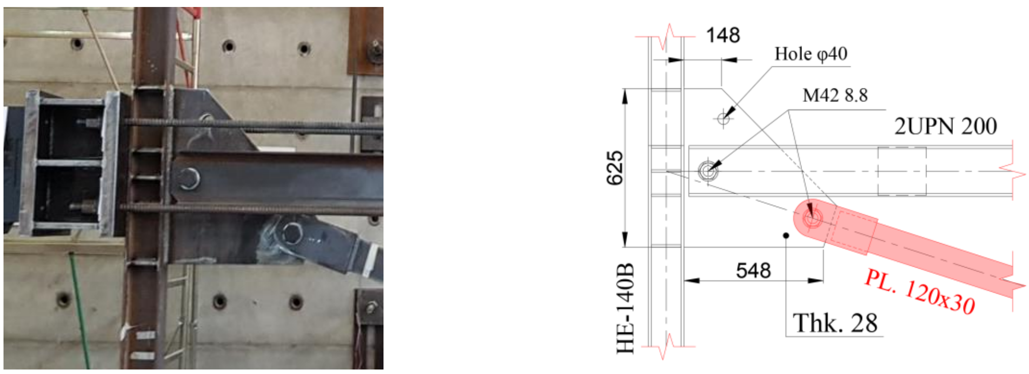


(a) (b)

Figure 3 - Steel connection plate of the CSB with the pendular frame: (a) picture, (b) geometric details.

## 4. Experimental setup and instrumentation for Configuration 1

For sake of conciseness, the present work focuses on the experimental results and interpretation of the test performed on Configuration 1 only.

In order to avoid out-of-plane displacements caused by instability, the frame has been connected to a stabilizing braced frame characterized by high out-of-plane lateral stiffness and strength (Figures 4a and b).



 

The lateral force is applied through a MTS hydraulic actuator anchored to a horizontal strong wall with a load capacity of 1000 kN in both directions (tension and compression) suitably constrained to the steel frame with a system of Dywidag bars that are able to transfer the load to the beam in the pull phase (Figures 4c, d, e, f).

The test instrumentation, fully detailed in Fig. 6, is defined with the purpose of monitoring the horizontal force applied by the actuator, the horizontal displacements at the two levels, as well as rotations and deformations of the elements constituting both the frame and the CSB devices.

Horizontal displacements at the base, at the floor level and at the top level were measured through inductive displacement transducers (LVDT) and potentiometers, with different measurement bases between 10 mm and 125 mm (Fig. 7a). The CSB devices have been equipped with six strain gauges to both the intrados and extrados of the braces, as well as Digital Image Correlation (DIC) technique, an image-based monitoring system able to acquire the full field of strain during the entire test (Fig. 6b). Strain gauges were attached at the mid-height of the column (along the neutral axis) in order to evaluate the state of tension of the frame during the test.

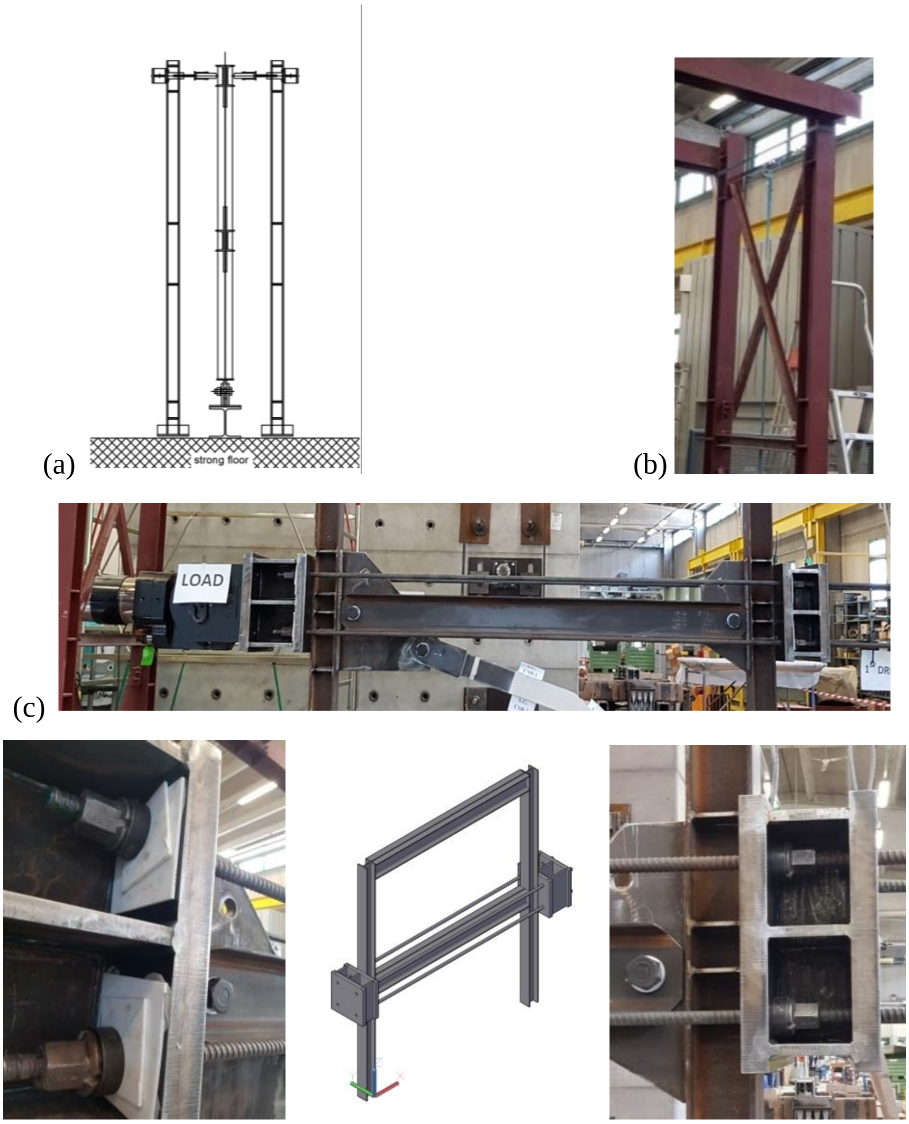


(a) (b) (c) (d) (e) (f)

Figure 4 - Details of the experimental setup: (a) scheme of the stabilizing braced frame, (b) picture of the stabilizing braced frame, (c) system of Dywidag bars to apply the load in the pull phase, (d) (e) (f) .



 

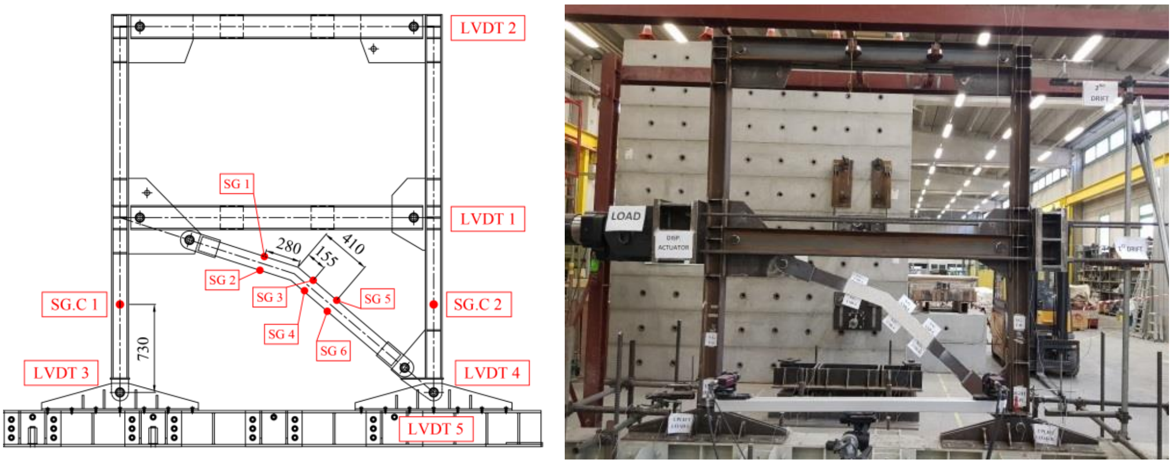


( a) (b)

Figure 5 - Instrumentation: (a) general scheme, (b) picture.

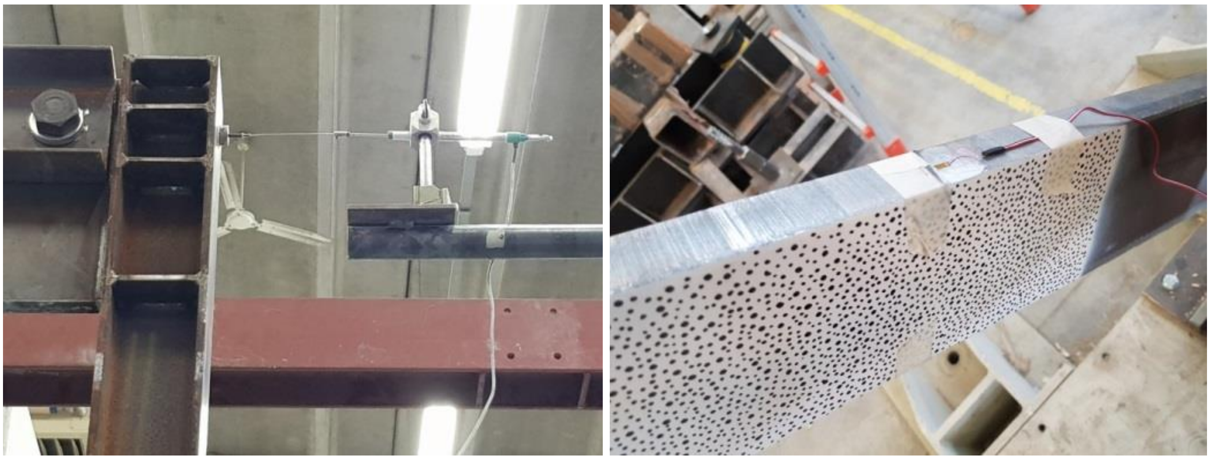

(a) (b)

Figure 6 - Details of the instrumentaion: (a) LVDT; (b) surface preparation for DIC and strain gauge position.

Quasi-static cyclic tests have been carried out following the requirements of UNI EN 15129 [14]. The testing protocols of UNI EN 15129 requires symmetric force-displacement cycles at amplitudes equal to 25%, 50% and 100% of the maximum displacement. For the tests performed, a maximum displacement equal to 50 mm is considered, corresponding to 3% of the inter-storey height, representative of a typical drift demand at ultimate limit state for a steel frame located in a high seismicity-risk zone. To avoid buckling during the compression phase in the CSB devices, the amplitudes of the cycles in compression have been reduced to half the amplitude in tension. Fig. 8 presents the nominal testing protocol adopted for the test on Configuration 1. The test is carried out in displacement control, having a displacement velocity varying between 0.1 and 0.3 mm/s. After cycle IX, a further cycle has been applied reaching a maximum displacement in tension of about 60 mm.



 

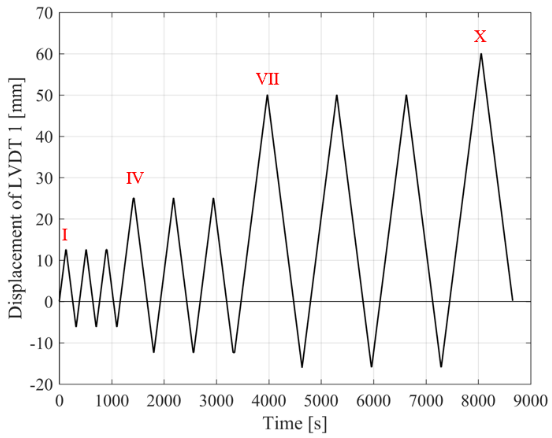


Figure 7 - Nominal testing protocol for Configuration 1.

## 5. Experimental results for Configuration 1

The present section describes the experimental results of Configuration 1 in terms of: (i) global force-displacement response (Section 5.1); (ii) energy dissipation capabilities of the CSB (Section 5.2); (iii) local deformations of the knee region of the CSB (Section 5.3).

### 5.1 Global response: force-displacement response

The global force-displacement response in terms of applied lateral force and lateral displacements at the first (LVDT 1) and second (LVDT 2) levels is presented in Fig. 8a. The displacement recorded at the second level is twice of the one recorded at the first level, thus confirming the expected pendular behavior of the pinned frame.

The maximum recorded lateral force was equal to 285 kN reached at Cycle X for a displacement equal to 60 mm, 14 mm of which are due to bolt/holes tolerances. The recorded cyclic response evidences good overall performance of the system with a stable cyclic behaviour, remarkable energy dissipation without noticeable stiffness reduction and strength degradation of cycles at the same level of imposed displacement. Pinching effect is observed due to bolt slip. No significant relative horizontal slip at the base and no uplift of the anchorage devices were recorded by LVDT 3 and 4 and by LVDT 5, respectively.

Figure 9b shows the tensile force-displacement envelope diagram for the first level (LVDT 1), upon which it is easy to identify the initial point (O: 14 mm, 10 kN) for which the CSB starts working, the first yielding point of the system (Y1: 32 mm, 175 kN) and the peak point achieved in the test (U: 60 mm, 285 kN). Initial stiffness of the CSB is around 9.2 kN/mm. It is then possible to construct, according to the common energy balance criterion, an idealised elasto-plastic relationship, that allows for the estimation of the equivalent yielding point (Y: 38 mm, 230 kN) and equivalent ductility capacity ($\mu = \delta_u / \delta_y = (60-14)/(38-14) = 1.92$).

Figure 9 shows the strains measured by the gauges SG.C 1 and SG.C 2 in the columns, that clearly indicate the expected behaviour of the pendular frame, i.e. right-hand column unloaded and left-hand column in the elastic phase.



 

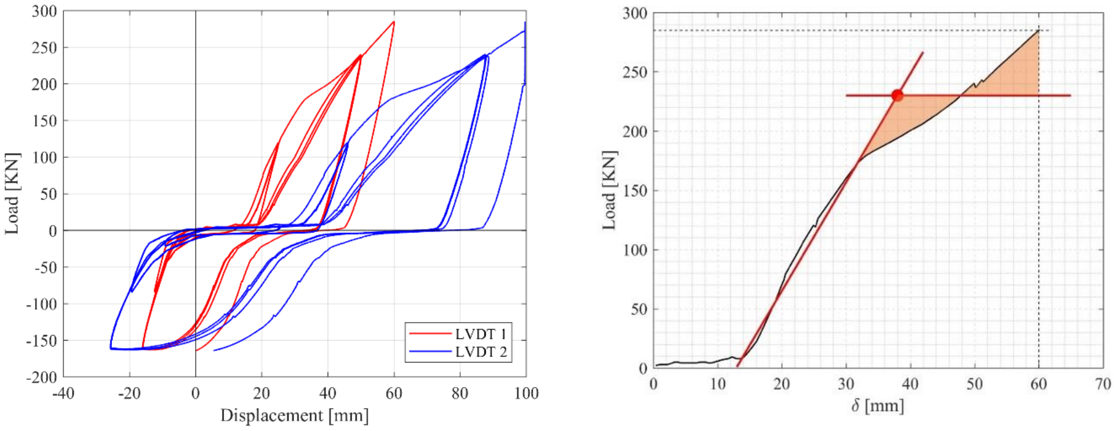


( a ) (b)

Figure 8 - Experimental results of Configuration 1: (a) global force-displacement response of the system; (b) tensile force-displacement envelope diagram.

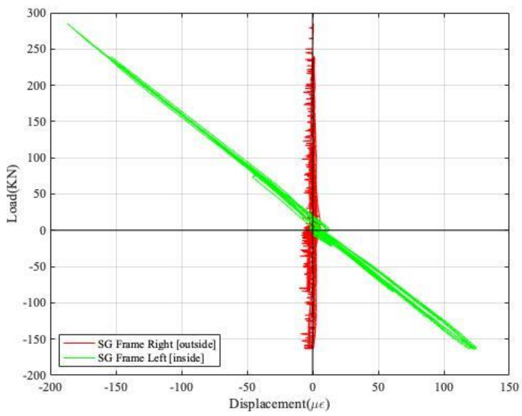


Figure 9 - Experimental results of Configuration 1: strain values in the columns.

## 5.2 Energy dissipation of the braced system

In order to evaluate the CSB energy dissipation capacity, the equivalent damping ratio $\xi_{eq,i}$ has been computed according to Jacobsen (1930), considering the $i^{th}$ half hysteretic cycle either in tension or compression, as follows:

$$\xi_{eq,i} = \frac{1}{\pi} \cdot \frac{A_{half,i}}{F_{\max,i} \cdot \Delta_{\max,i}} \tag{1}$$

where $A_{half,i}$ is the energy dissipated by the CSB in the $i^{th}$ half hysteresis cycle; $F_{max,i}$ and $\Delta_{max,i}$ are the maximum recorded force and displacement amplitude for the $i^{th}$ half cycle, respectively (Fig. 11).

The equivalent damping ratio has been computed for each half cycle in tension and compression, computing the corresponding area as depicted in Figure 10. The overall results in terms of equivalent damping ratio and maximum imposed drift are presented in Figure 11. For both tension and compression, an average value of 8 to 10% of damping ratio is reached for the highest cycles. These results are in line with the first investigations carried out on 1:6 scaled CSB devices presented in (Palermo et al 2017).



 

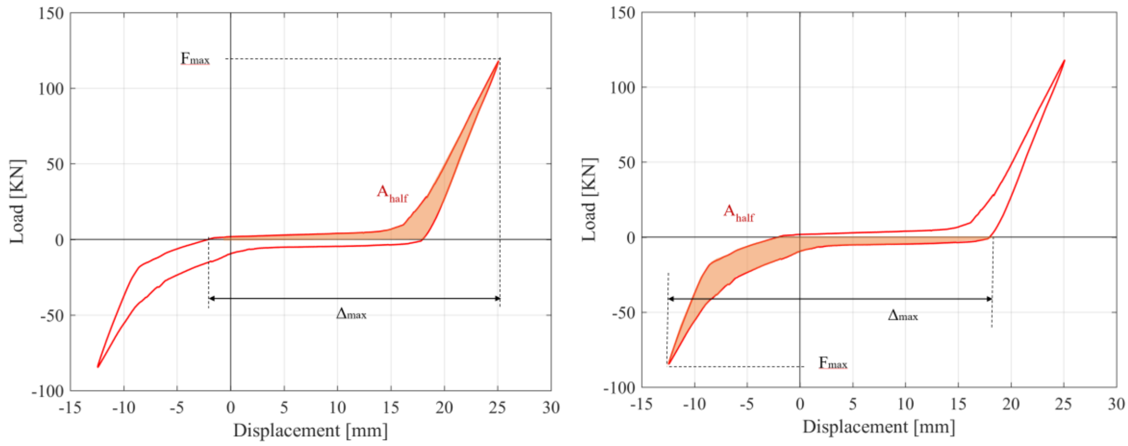


(a) (b)

Figure 10 - Cyclic energy dissipation capacity calculation shown on one cycle: (a) tension, (b) compression.

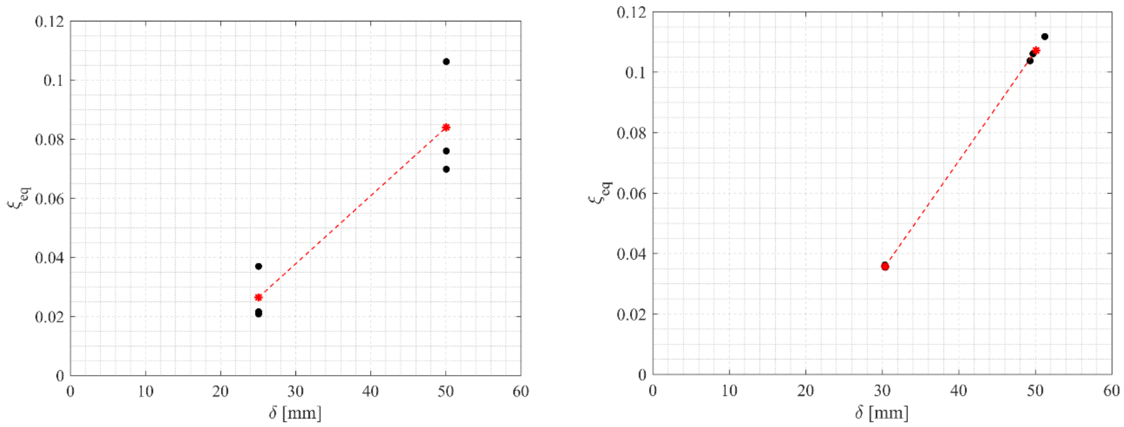


(a) (b)

Figure 11 - Equivalent damping ratios for Configuration 1 in different half cycles: (a) tension, (b) compression.

## 5.3 Local response: strain-gauges results and DIC results

The local response has been monitored by means of both strain gauges and DIC. Figures 12a and b display colored maps of the strain field as obtained from the DIC outputs corresponding to the two specific points of the force-displacement response at which maximum tensile and compressive force are reached (cycle X for tension and cycle IX for compression).

Fig. 13a displays the strains as recorded by the six strain gauges vs the applied lateral load. The vertical dotted black lines indicate the yielding strain. It can be noted that the values of all recorded strains exceeded yielding. Maximum recorded strains are about 1.5%.

From the whole strain field as obtained from DIC, it is possible to evaluate strain values at specific locations. In particular, the Figures 13a and b compare the results from strain gauges and the corresponding "virtual strain gauges" taken from the DIC outputs at the same locations. It can be appreciated that at first approximation the two systems provide similar results.



 

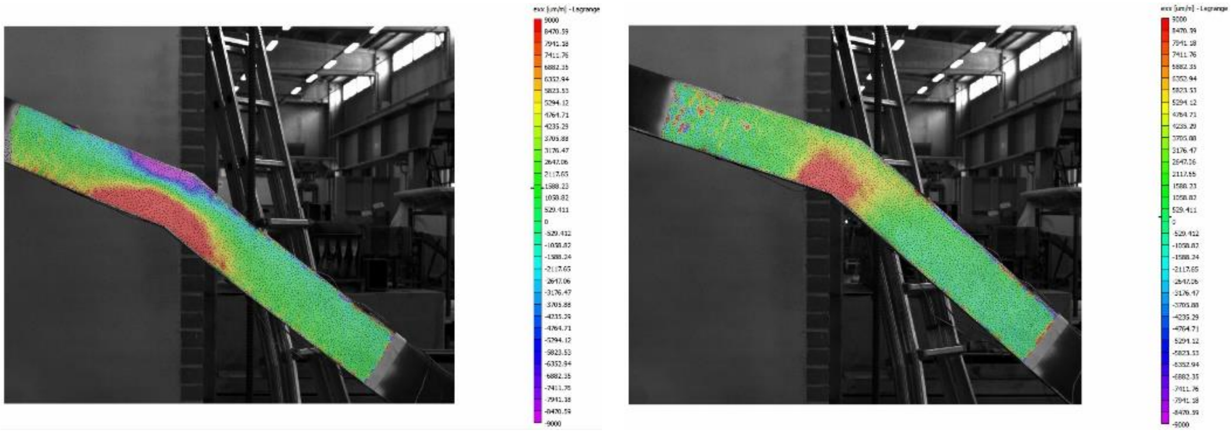

(a) (b)

Figure 12 - DIC outputs: (a) maximum tensile force (cycle X); (b) maximum compression force (cycle IX).

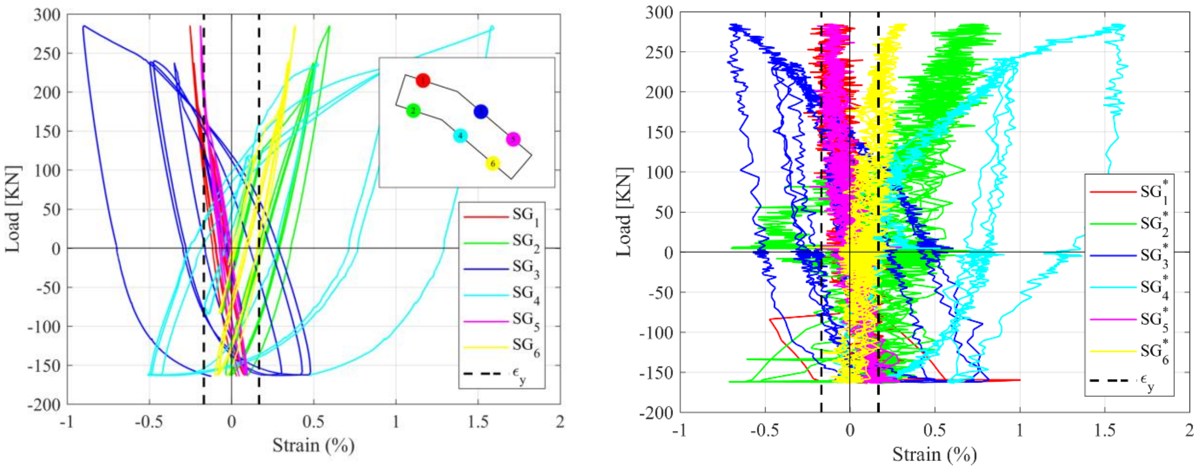


(a) (b)

Figure 13 - Comparison of strain gauges measurements and DIC outputs: (a) local response of the strain gauges located on the CSB vs. (b) virtual strain gauges" taken from the DIC outputs at the same locations.

A detailed inspection of the strain histories as recorded by the six strain gauges allows to identify the "first yielding point" of the CSB device, corresponding to the point in the force-displacement response when the strain gauge exceeds yielding strain for the first time. Figure 14 highlights the first yielding point at each strain gauge. The first strain gauge that reached yielding is SG2, at cycle IV (corresponding to a maximum amplitude of 50% the ultimate displacement), while the remaining five reached yielding point at cycle VII (corresponding to the first cycle at maximum amplitude of 100% the ultimate displacement). For all six strain gauges yielding occurred for applied force between 120 and 180 kN, with an average of 150 kN, and for a horizontal displacement of the control point (which corresponds to the first floor for Configuration 1) between 25 and 35 mm, with an average of 30 mm.



 

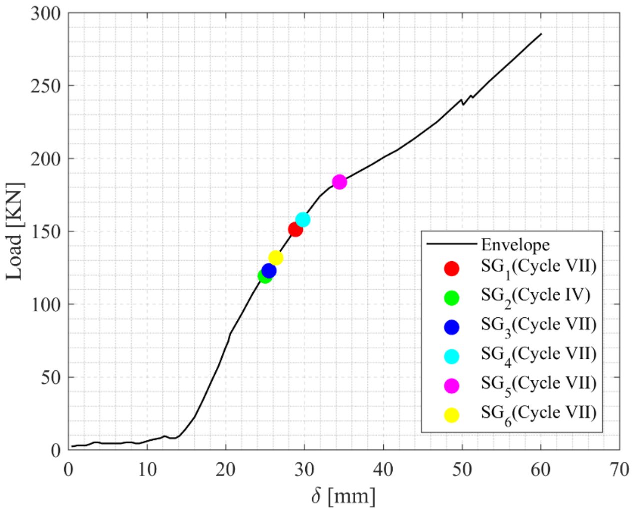


Figure 14 - Envelope diagram with first yielding points of strain gauges.

## Conclusions

The work presents and discusses the main experimental results of pseudo-static cyclic tests performed on a half-scaled two-storey steel frame equipped with Crescent Shaped Braces (CSB hysteretic dissipative bracings. The brace has a boomerang-like shape able to satisfy selected performance objectives during the design phase, through the definition of suitable geometrical parameters. The response of the device is highly influenced by both mechanical and geometrical non-linearity.
The experimental tests have been performed under quasi-static loading conditions, following the cyclic protocol as of UNI EN 15129. The maximum imposed lateral drifts correspond to the 3% of the inter-storey height. Two different configurations have been studied: (1) frame equipped with a single CSB device at the first storey only; (2) frame equipped with two CSB devices, one for each storey. This paper focuses on the results of the second configuration.
Both the frame and the CSB have been equipped with different measuring systems, in order to capture both global and local (punctual) response during the test. In particular, the frame deformation has been measured through LVDTs, whereas local information on the CSB devices has been taken by means of strain gauges and Digital Image Correlation system.
During the test the brace was able to carry a maximum lateral force in tension of around 300 kN with a displacement capacity of around 60 mm, corresponding to a displacement ductility of around 2.0. Overall, the cyclic behaviour evidenced good performances associated to a stable cyclic behaviour, remarkable energy dissipation without noticeable stiffness reduction and strength degradation. The observed pinching effect was attributed to bolt slip. The equivalent damping ratio has been estimated in the order of 10%. The energy dissipation was due to the local plasticisation of the knee point with maximum strains of around 1.5%. The experimental behaviour of the CSB inserted in a frame structure was in line with expectations, thus confirming the capabilities of CSB in achieving the desired seismic performances.

## Acknowledgements

Financial supports of Department of Civil Protection, University of Bologna within the “TIRISICO POR-FESR 2014-20020 project” Regional Research Project is gratefully acknowledged.



 

The Effebi company for the support provided in the design and construction phase of the test frame and CSB devices is thanked.
We are also grateful to the colleagues Tomaso Trombetti and Giada Gasparini for their support in the first stages of the design of the frame to be tested, and to Claudio Mazzotti, Andrea Incerti and Diterihs Erra (CIRI Building & Construction) for their support and experience for the test setup and during the laboratory activities.
Finally, Vincenzo Saffioti is also thanked for his precious help during the tests.

## References

[1] Eurocode 8: Design of structures for earthquake resistance -Part 1: General rules,seismic actions and rules for buildings, Brussels: CEN national Members, 2004.

[2] "Journal of the seismic rehabilitation of existing buildings 360-2006 instructions," Department of Engineering Management and Planning, 2006.

[3] Tomaso Trombetti, Giada Gasparini, Stefano Silvestri and Ilaria Ricci, "Use of Crescent Shaped Braces for Controlled Seismic Design of Ductile Structures," Journal of Civil Engineering and Architecture, vol. 5, no. 10, pp. 890-902, 2011.

[4] Palermo M, Ricci I, Gagliardi S, Silvestri S, Trombetti T, Gasparini G, "Multi-performance seismic design through an enhanced first-storey isolation system," Engineering Structures, vol. 59, p. 495–506, 2014.

[5] Andrew Charleson, Seismic Design for Architects, Outwitting the Quake, Architectural Press, imprint of Elsevier, Linacre House, Jordan Hill, Oxford OX28DP, UK, first Edition, 2008.

[6] C. Christopoulos, A. Filiatrault, Principles of Passive Supplemental Damping and Seismic Isolation, Pavia: IUSS Press, 2006.

[7] Robinson, W., & Greenbank, L., "An extrusion energy absorber suitable for the protection of structures during an earthquake.," Earthquake Engineering & Structural Dynamics, vol. 4, no. 3, pp. 251-259, 1976.

[8] Trombetti T, Silvestri S, Gasparini G, Ricci I, "Stiffness-strength-ductility-design ap-proaches for crescent shaped braces," Open Constr Build Technol , vol. 3, p. 127–40, 2009.

[9] Khan, F., Fintel, M., “Shock-absorbing soft story concept for multi-story earthquake structures”, ACI Journal, **65**(5), 1968.

[10] Palermo, M., Silvestri, S., Gasparini, G., Trombetti, T., "Crescent shaped braces for the seismic design of building structures," Materials and Structures, **48**(5), 1485–1502, 2014.

[11] Palermo, M., Pieraccini, L., Dib, A., Silvestri, S., Trombetti, T., "Experimental tests on Crescent Shaped Braces hysteretic devices," Engineering Structures, **144**, 185-200, 2017.

[12] Kammouh, O., Silvestri, S., Palermo, M., Cimellaro, G.P., "Performance-based seismic design of multistory frame structures equipped with crescent-shaped brace," Structural Control and Health Monitoring, **25**(2), 2017.

[13] Bertero RD, Bertero V V. “Performance-based seismic engineering: The need for a reliable conceptual comprehensive approach”. Earthq Eng Struct Dyn 2002;31:627–52. https://doi.org/10.1002/eqe.146.

[14] UNI EN 15129, “Anti-seismic devices”, 2009.



 